ROYAL SOCIETY OF CHEMISTRY

Amperometric cholesterol biosensor based on zinc oxide films on a silver nanowire–graphene oxide modified electrode

Qiong Wu,*[a] Yiting Hou,[b] Mengdan Zhang,[a] Xiaochun Hou,[b] Lin Xu,[cd] Nana Wang,[a] Jianpu Wang[a] and Wei Huang[a]

A highly sensitive and selective cholesterol biosensor is successfully fabricated in this work. Due to excellent conductivity and catalytic activity, silver nanowires (AgNWs) and zinc oxide (ZnO) are modified on an indium tin oxide (ITO) electrode with graphene oxide (GO) and chitosan (CS) to construct the novel amperometric biosensor. The composite of AgNW–ZnO successfully enhanced electron communication, and the electrochemical performances of the ChOx/ZnO/Ag/GO–CS/ITO electrode were investigated via scanning electron microscopy (SEM), cyclic voltammetry (CV) and impedance measurements. The linear response to cholesterol in the range of the fabricated biosensor is 0.25–400 mg dL^{-1} (6.5 µM to 10 mM) with a sensitivity of 9.2 µA µM^{-1} cm^{-2}. Moreover, the limit of detection (LOD) is 0.287 µM (S/N = 3), and the Michaelis–Menten constant is calculated to be about 0.295 µM in 0.1 M phosphate buffer solution (pH 7).

Introduction

Cholesterol is an adipic substance which can be widely found in organisms. It contributes to constituting plasma membranes and protecting mammalian cells from foreign matter.[1] The total cholesterol level in a healthy person's serum should be lower than 200 mg dL^{-1} (5.2 mM). A high cholesterol level may lead to fatal diseases, such as atherosclerosis, cerebral thrombosis, coronary heart diseases and myocardial infarction.[2] Therefore, developing a highly sensitive biosensor for cholesterol analysis is important in clinical diagnosis. The key to the question is how to detect the concentration of cholesterol.

Recently, in order to meet the needs of patients, cholesterol estimation techniques have been developed at a fast pace. Many methods can be used to detect cholesterol in blood plasma such as fluorometry,[3] high performance liquid chromatography,[4] and electrochemical methods.[5] Electrochemical biosensors are accurate, speedy and convenient. In order to analyze cholesterol, electrochemical assays requiring the use of specially modified electrodes have attracted great attention of more and more researchers.

Most cholesterol biosensors are developed based on the electrochemical reduction of hydrogen peroxide (H$_2$O$_2$). For example, cholesterol oxidase (ChOx) and horseradish peroxidase (HRP) are modified on the biosensor, which yields H$_2$O$_2$ and performs the redox production of cholesterol (cholest-4-en-3-one) via an enzymatic reaction.[6] Hence, improving the enzyme activity is one of the most attractive methods for monitoring cholesterol.

In our previous work, we fabricated a nonenzymatic cholesterol sensor based on silver nanowires (AgNWs) to improve the electrocatalytic activity of the reduction of H$_2$O$_2$.[7] AgNWs have many remarkable properties such as large surface to volume ratios, high conductivity, good surface reaction activity and catalytic activity.[8] This friendly microenvironment of one-dimensional (1-D) nanomaterials is not only helpful to enhance the adsorption ability of biomolecules, but also beneficial to facilitate electron transfer in biosensors.[9] These low-cost materials are ideal candidates for the development of electrochemical sensors.

The metal–semiconductor zinc oxide (ZnO) and its 1D nanostructure also have attracted great interest in biosensing applications due to its unique properties like nontoxicity, biocompatibility, superior surface area, high chemical stability, good electrochemical activities, enhanced sensitivity, low cost and so on.[10] Wide bandgap ZnO nanocrystals (E_g = 3.37 eV) with high electron mobility may exhibit excellent efficient electron transport in the development of electrochemical sensors. In addition, ZnO nanocrystals have a high isoelectric point (IEP) of

[a]Key Laboratory of Flexible Electronics (KLOFE) & Institute of Advanced Materials (IAM), National Jiangsu Synergistic Innovation Center for Advanced Materials (SICAM), Nanjing Tech University (NanjingTech), 30 South Puzhu Road, Nanjing 211816, China. E-mail: iamqwu@njtech.edu.cn

[b]Key Laboratory for Organic Electronics & Information Displays (KLOEID), Nanjing University of Posts and Telecommunications, Nanjing 210046, China

[c]State Key Laboratory of Materials-Oriented Chemical Engineering and College of Science, Nanjing Tech University (NanjingTech), 30 South Puzhu Road, Nanjing 211816, China

[d]Nanjing Vocational Institute of Science and Technology, 625 GeGuan Road, Nanjing 210048, China

9.5, which is helpful for the immobilization of low biomaterials (protein, enzyme) such as ChOx (IEP $\sim$ 5.0) in buffer solutions *via* strong electrostatic binding.[11]

The combination of ZnO nanocrystals with AgNWs helps it to keep its surface area.[12] Furthermore, the composite of ZnO–noble nanometals enhance the catalytic activity, which is crucial for the fabrication of biosensors.

Graphene oxide (GO) acts as an advanced transducer to enhance the sensitivity of cholesterol sensors owing to its outstanding electronic properties and unique surface suitable for chemical modification chemistry.[13] Chitosan (CS) acts as a conductive bridge between AgNWs and ZnO to solidly immobilize AgNWs on the surface of electrodes.[14] The GO–CS nanocomposite membrane is considered as a good candidate to strengthen the catalytic activity of AgNWs. This approach is conducive to realizing better performances for amperometric cholesterol biosensors.

In this work, ZnO nanocrystals are spin-coated over AgNWs and a GO–CS membrane. As illustrated in Scheme 1, a highly sensitive cholesterol biosensor is fabricated by integrating several high-performance materials.

Experimental

Materials

Ethylene glycol, poly(vinyl pyrrolidone), silver nitrate, zinc acetate hydrate, graphene oxide, chitosan, dimethyl sulphoxide (DMSO), tetramethylammonium hydroxide (TMAH), ethyl acetate, ethanol, 2-ethanolamine, isopropanol, sodium phosphate dibasic, sodium phosphate monobasic, potassium hexacyanoferrate, potassium ferricyanide, and potassium chloride were purchased from Sigma-Aldrich. The double distilled water was used to prepare all experiments. All other chemicals were of analytical grade and used without further purification.

Preparation of AgNWs

The aspect ratio-controlled AgNWs were synthesized according to a reported procedure.[15] 10 mL of silver nitrate (0.10 g AgNO$_3$ dissolved in 10 mL ethylene glycol (EG)) was added in a stirred mixture solution of 10 mL of EG and 0.40 g of poly(vinyl pyrrolidone) (PVP, K30). 1 mL of an AgNO$_3$ solution was treated to obtain the Ag crystal seeds in the first 3–5 min. Then a successive 9 mL of an AgNO$_3$ solution was added using a syringe. After the solution turned into a grey emulsion, it was continuously boiled for half an hour. Finally, the emulsion was cooled down

to room temperature. Almost all AgNWs were deposited at the bottom of flask after one day.

Preparation of ZnO nanocrystals

Colloidal ZnO nanocrystals were synthesized as we described previously.[16] Briefly, 3 mmol of zinc acetate hydrate (in 30 mL DMSO solution) was mixed with 5.5 mmol of TMAH (in 10 mL ethanol solution) and stirred for 2 h at room temperature. The resulting ZnO nanocrystals were precipitated due to the addition of ethyl acetate. The redispersion of ZnO nanocrystals was treated with ethanol. The above purification step was repeated twice, and then 160 μL of 2-ethanolamine was added to form the surface ligands of the ZnO nanocrystals. 0.22 μm of a PTFE filter was used to ensure the purity of the ZnO nanocrystals.

Fabrication of the cholesterol biosensor

A sheet of ITO glass was cleaned using an ultrasonic cleaning machine and dried in a nitrogen gas flow. Firstly, 0.5 mg mL^{-1} GO–CS (5 μL) mixed solution was spread on the ITO-coated glass substrates and dried at room temperature. Then, the dried electrodes were immersed in the AgNW solution for 5 min, and dried under nitrogen to form the Ag/GO–CS/ITO modified electrode. After that, solutions of ZnO nanocrystals (80 μL) were spin-coated onto the Ag/GO–CS/ITO electrode surface (3000 rpm, 40 s). As noted, the obtained electrode is ZnO/Ag/GO–CS/ITO. For the detection of cholesterol, ChOx was placed on the modified electrode and dried at 4 °C. The fabrication process of the ChOx/ZnO/Ag–GO–CS/ITO electrode is shown in Scheme 1.

Apparatus

The morphological characterization of the nanomaterials and the modified electrode surface was obtained *via* scanning electron microscopy (SEM, Hitachi S-4800, Japan) and transmission electron microscopy (TEM, HT7700, Hitachi, Japan). UV experiments were performed using a PerkinElmer spectrometer (Lambda 35 650s, USA). The entire electrochemical measurements such as cyclic voltammetric (CV), amperometric and impedance measurements were carried out using an Autolab302N electrochemical workstation (Metrohm Autolab, The Netherlands) with a conventional three-electrode system. The modified ChOx/ZnO/Ag/GO–CS/ITO electrode was used as the working electrode; a platinum coil and an Ag/AgCl (saturated KCl) electrode were used as counter electrode and the reference electrode, respectively.

Results and discussion

Materials characterization

Scanning electron microscopy (SEM) and UV-spectrometry are helpful to identify the micro structure of the AgNWs (Fig. 1a and b). Fig. 1a shows that the high purity AgNWs are successfully synthesized with an average diameter of 50 nm, and a long length (45 ± 5 mm). The absence of the 410 nm peak illustrates a very pure AgNW solution without Ag nanoparticles. And the typical absorption spectra of the AgNWs are at 350 nm and 390
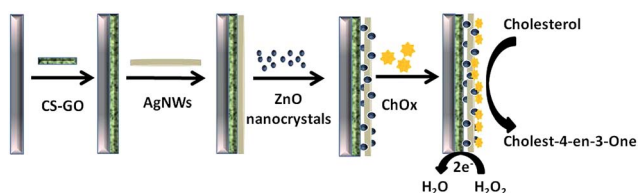
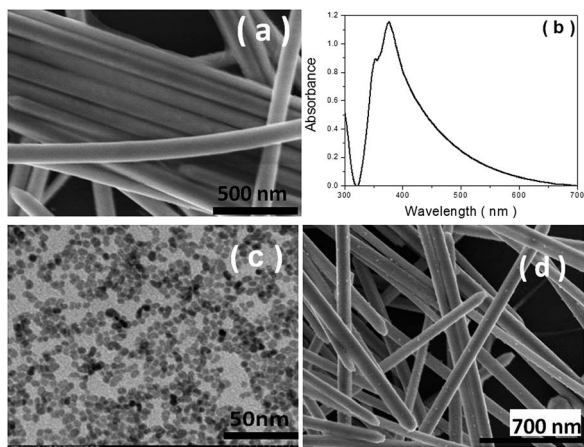**Scheme 1** The schematic diagram of the preparation process of cholesterol biosensor.

Fig. 1 The SEM image of the AgNWs (a); UV-vis absorption spectra of the AgNWs (b); TEM images of the ZnO nanocrystals (c); and ZnO/AgNWs on the modified ITO electrode (d).

nm (Fig. 1b). The uniform morphology of the ZnO nanocrystals is examined *via* TEM (Fig. 1c). It obviously shows the well dispersed ZnO nanocrystals with an average diameter of 5 nm. The specific area of ZnO nanocrystals is of great benefit for electron transport.

The surface morphology of the ZnO/Ag/GO–CS/ITO electrode is analyzed *via* SEM. Fig. 1d shows the characterization of the biosensor fabrication process in the absence of ChOx. When ZnO nanocrystals were spin coated on top of the AgNWs, the surface of the AgNWs showed tiny particles, which indicated that ZnO nanocrystals were successfully adsorbed to the surface of the AgNWs.

Electrochemical properties

Cyclic voltammetry is a unique technique to investigate the electrocatalytic behavios of electrode materials. The modified electrodes are electrochemically characterized in 10 mM PBS and a 200 mg dL^{-1} cholesterol solution (pH 7.0) *via* CV, as shown in Fig. 2. The CV spectra in the present study are recorded in the range from -0.8 V to 0 V at a scan rate of 50 mV s^{-1}.
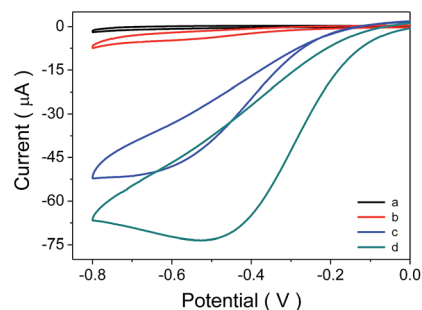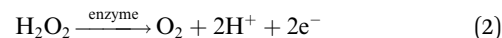

Fig. 2 Cyclic voltammograms of different electrodes: (a) naked ITO in PBS solution (pH 7.0); (b) ChOx/ZnO/ITO; (c) ChOx/Ag/GO–CS/ITO; (d) ChOx/ZnO/Ag/GO–CS/ITO in the presence of a 200 mg dL^{-1} cholesterol solution (pH 7.0) with a scan rate at 50 mV s^{-1}.

Cholesterol is oxidized by ChOx to cholest-4-en-3-one in the presence of oxygen, while ChOx is changed into its reductant, ChOx (reduction, Reaction (1)). As a result, H_2O_2 is produced and then catalyzed by AgNWs (Reaction (2)). As indicated here:

$$Cholesterol + O_2 \xrightarrow{ChOx} cholest\text{-}4\text{-}en\text{-}3\text{-}one + H_2O_2 \quad (1)$$

$$H_2O_2 \xrightarrow{enzyme} O_2 + 2H^+ + 2e^- \quad (2)$$

The results obtained are shown in Fig. 2, the corresponding cyclic voltammetric of the naked ITO electrode in PBS (curve a) and the ChOx/ZnO/ITO electrode in cholesterol solution (curve b) do not display obvious redox peaks.

AgNWs are known to catalyze the dissociation of H_2O_2 to electrons (Reaction (2)). In earlier work, we investigated the behavior of GO which would improve the performances of AgNWs.[7] When AgNWs were coated onto a GO–CS modified ITO electrode, an enhancement in the peak current can be seen in curve c. This can be attributed to the presence of AgNWs and GO–CS promoting the electrocatalytic activity and expanding the reaction area. Due to the positively charged ZnO nanocrystals available to promote the electron transfer between the negatively charged enzyme (AgNWs) and the electrodes, the ZnO nanocrystal-modified ChOx/ZnO/AgNWs/GO–CS/ITO electrode (Fig. 2, curve d) shows a cathodic peak centered at a lower negative potential (-0.47 V) when compared to the ChOx/AgNWs/GO–CS/ITO electrode in 200 mg dL^{-1} cholesterol solution (Fig. 2, curve c).[17] Comprehensively, the significant changes in the performance of current responses owing to ZnO nanocrystals may act as electron transfer media, which quite efficiently optimized the amperometric response towards cholesterol. As a result, the ChOx/ZnO/AgNWs/GO–CS/ITO electrode is found to be electroactive for the catalytic activity of cholesterol.

As is well known, potassium ferrocyanide/potassium ferricyanide is often used as an electron transfer rate probe for surface characterization. In this study, the stepwise assembly process of the electrode is investigated using the $[Fe(CN)_6]^{3-/4-}$ electrochemical probe and *via* electrochemical impedance spectroscopy (EIS). EIS is an effective method for studying the charge transfer properties of the electrode interface. The semicircle diameter of the impedance equals the electron transfer resistance (R_{et}), which controls the electron transfer kinetics of the redox probe at the electrode interface. A linear portion at a lower frequency range shows a controlled diffusion process. The Randles equivalent circuit is shown in Fig. 3 (inset). It can be used to measure impedance values which consists of a solution resistance (R_s) in series with a charge transfer resistance (R_{ct}) in parallel with a double-layer capacitance (C_{dl}).

Fig. 3 presents the impedance spectrum of each modified stage. Compared with bare ITO (curve a), when AgNWs are modified on the electrode (curve b), the Nyquist semicircle becomes larger due to non-conductive GO–CS as an adhesive that hinders electron transfer. In the presence of ZnO nanocrystals, the ZnO/AgNWs/GO–CS/ITO electrode (curve c) exhibits
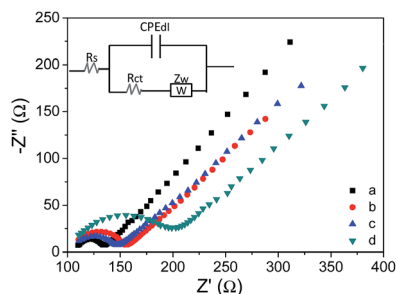
Fig. 3 Impedance spectra of the modified electrodes with different modification steps. Curve a: naked ITO, curve b: Ag/GO–CS/ITO, curve c: ZnO/Ag/GO–CS/ITO, and curve d: ChOx/ZnO/Ag/GO–CS/ITO.

a smaller Nyquist semicircle compared to the AgNW layer, which is attributed to the high conductivity of the ZnO–AgNWs composites. An amount of ChOx spreads onto the modified electrode; the Nyquist semicircle became the largest because of the non-conductive ChOx. The different curves of the impedance spectrum show that the modified materials are successfully immobilized onto the electrode. Besides, the low electron transfer resistance indicates that a diffusion-limited process occurs between the surface and the solution.

Electrochemical characterization of ChOx/ZnO/Ag/GO–CS/ITO

The electrochemical behavior of ChOx/ZnO/Ag/GO–CS/ITO was carried out in 5 mM potassium ferricyanide solution (pH 7.0) (Fig. 4). The ChOx/ZnO/Ag/GO–CS/ITO electrode displays a steady current response. With increasing scan rate, the redox
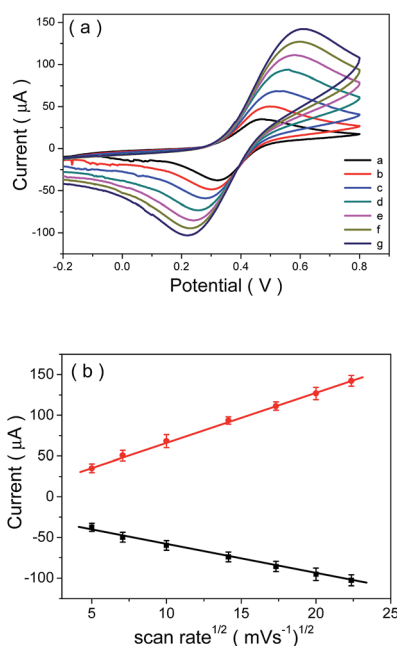

Fig. 4 Cyclic voltammograms of the ZnO/Ag/GO/CS/ITO electrode at 25–500 mV s^{-1} scan rates (curves a–g) in 5 mM potassium ferricyanide solution (a) and the relationship between the square root of the scan rate ($\nu^{1/2}$) and the peak current measured (b).

peak potential separation increased slowly, which indicated the limitation arising from charge transfer kinetics. Meanwhile, with increasing scan rate, the redox peak currents of ChOx/ZnO/Ag/GO–CS/ITO increased. The electrons migrated from the redox center of ChOx to the ZnO/Ag/GO–CS modified electrode. The impact of the proton gradient depends on the electron transfer between the aforementioned two layers. At high scan rates, both the anodic and cathodic potentials shifted, which may be attributed to the result of quantized double layer charging or due to the remarkable charge efficiency of the ZnO nanocrystals.[18]

From Fig. 4, both the anodic and cathodic peak currents of ChOx/ZnO/Ag/GO–CS/ITO are linearly proportional to the square root of the scan rate in the range of 25–500 mV s^{-1}, indicating that the electron transfer process for ChOx/ZnO/Ag/GO–CS/ITO was a diffusion confined electrode process. It is in agreement with Laviron's theory.[19] According to Laviron's equation, $I_p = nFQ\nu/4RT$, where n is the number of electrons, F is the Faraday constant, Q is the integrated charge of reduction peak, ν is the scan rate, R is the molar gas constant and T is the thermodynamic temperature. The value of n was calculated to be 2.0.

The ChOx/ZnO/Ag/GO–CS/ITO biosensor was used to measure cholesterol at different concentrations, and the amperometric responses were recorded. In order to increase the sensitivity, amperometry under stirred conditions were selected, hence the amperometric experiments have been performed at a constant potential of −0.47 V and under continuous stirring. The amperometric responses and calibration curves for the biosensor under the optimized experimental conditions are shown in Fig. 5. The biosensor exhibited linear ranges for cholesterol determination ranging from 0.25 mg dL^{-1} up to 400 mg dL^{-1} (6.5 μM to 10 mM) with excellent regression coefficients of $R = 0.9959$. The biosensor exhibited a rapid response to the changes in cholesterol concentration, and a stable current was obtained. The detection limit was estimated to be about 0.287 μM (S/N = 3), and the sensitivity of 9.2 μA μM^{-1} cm^{-2}.

The low apparent Michaelis–Menten constant (K_M^{app}) 0.295 μM indicates the high affinity of the ChOx/ZnO/Ag/GO–CS/ITO electrode to cholesterol. It gives an indication of the enzyme–substrate kinetics, which can be estimated from the Lineweaver–Burk equation as follow:[20]

$$1/I = 1/I_{max} + K_M^{app}/I_{max}[S]$$

where I is the steady-state current, I_{max} is the maximum current measured for the enzymatic product when electrode surface is saturated, and [S] is the concentration of cholesterol.

The fabricated biosensor exhibits higher sensitivity than the previously reported ChOx based cholesterol biosensors, and a summary is shown in Table 1.

Selectivity of the cholesterol sensor

Apart from sensitivity, an excellent bio-chemical sensor should possess a good anti-interference ability. It is well-known that many biocomponents are present in serum and interfere in the
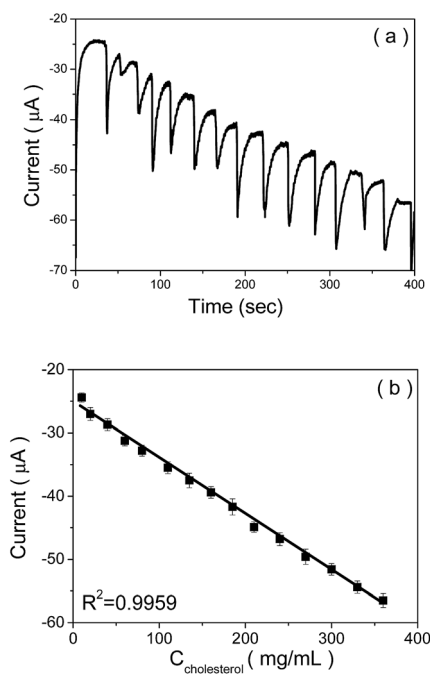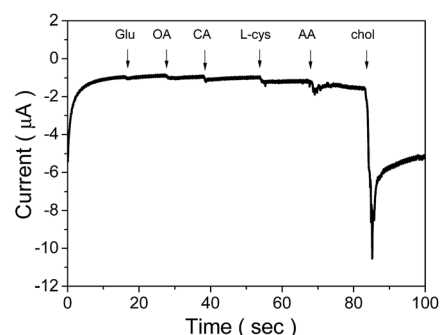
Fig. 6 Amperometric response of the interference test for the ChOx/ZnO/Ag/GO–CS/ITO electrode in phosphate buffer (pH 7.0) at a potential of −0.50 V with the addition of 0.1 M glucose, OA, CA, L-Cys and AA.

the above results illustrate that the ChOx/ZnO/Ag/GO–CS/ITO bio-electrode has a good selective response to cholesterol.

Reproducibility and stability

The reproducibility and stability of the ChOx/ZnO/Ag/GO–CS/ITO electrode were also investigated. The reproducibility was tested 8 times in a 200 mg dL^{-1} cholesterol solution using the CV technique. The relative standard deviation was 2.7%. Furthermore, we used eight different modified electrodes to determine 200 mg dL^{-1} cholesterol which showed a good reproducibility with a relative standard deviation (RSD) of 2.3%. The experiment was carried out to evaluate the reproducibility of the ChOx/ZnO/Ag/GO–CS/ITO electrodes which has been shown in Fig. 7a. Moreover, the stability of the ChOx/ZnO/Ag/GO–CS/ITO electrode was explored through measuring the current response during the reduction of cholesterol using the modified electrode. The change in the CV curves of the ChOx-modified ZnO/Ag/GO–CS/ITO electrode for 30 days is shown in Fig. 7b. It was found that the response value decreased by about 2.1% in 10 days, and 4.7% in 30 days, which indicated that the modified electrode had good stability.

Fig. 5 (a) Amperometric response of the cholesterol solution at the ChOx/ZnO/Ag/GO–CS/ITO modified electrode in phosphate buffer (pH 7.0) at a −0.47 V constant potential and 1000 rpm rotation speed; (b) the plot of the catalytic current of the ChOx/ZnO/Ag/GO–CS/ITO electrode vs. the concentration of cholesterol solution.

detection of cholesterol when using a biosensor. Therefore, to explore the selectivity of the ChOx/ZnO/Ag/GO–CS/ITO bio-electrode, some electroactive species such as glucose (Glu), oxalic acid (OA), citric acid (CA), L-cysteine (L-Cys), ascorbic acid (AA) and cholesterol (chol) are introduced into the PBS solution (pH 7.0). The effect of the interferents is investigated through the current–time responses of the prepared electrode (Fig. 6). At an applied potential of −0.5 V with a scan rate of 50 mV s^{-1}, a significant current increment cannot be observed even when the amounts of interferent are up to 20 times greater than cholesterol concentration (200 mg dL^{-1}, 5.2 mM). Thus, all of

Table 1 Comparison of the ChOx/ZnO/Ag/GO–CS/ITO biosensor with other ChOx based biosensors[a]

Electrode	Linear range	Sensitivity	References
ChOx/(ZnO–CuO)/ITO/glass	0.12–12.93 mM	680 μA mM^{-1} cm^{-2}	18
L–MMT/ITO	1–20 mM	0.518 μA mM^{-1} cm^{-2}	21
ITO(PEI/Hb)$_5$(PEI/COx)$_{10}$	0–7.4 mM	93.4 μA μM^{-1} cm^{-2}	22
ChOx/nanoZnO–CS/ITO	0.1–7.7 mM	5.45 mA mM^{-1}	23
Si/Ag/ZNT/ChOx/Nafion	1.0 μM to 13.0 mM	79.40 μA mM^{-1} cm^{-2}	24
NiO/CVD-grown graphene	2–40 μM	40.6 mA μM^{-1} cm^{-2}	25
Laponite/IL/ITO	1–20 mM	8.0 μA mM^{-1} cm^{-2}	26
ChOx–ChEt/CS–CdS/ITO	0.64–12.9 mM	0.384 μA mM^{-1} cm^{-2}	27
ChOx/pRGOSHs/ITO	2.6–15.5 mM	11.1 μA mM^{-1} cm^{-2}	28
ChEt–ChOx/MWCNT/SiO$_2$–CS/ITO	0.25–13 mM	0.95 μA mM^{-1} cm^{-2}	29
ChOx/PAni–Au–CS/ITO	1.3–13 mM	33.26 μA mM^{-1} cm^{-2}	30
ChOx/ZnO/Ag/GO–CS/ITO	6.5 μM to 10 mM	9.2 μA μM^{-1} cm^{-2}	This work

[a] L: Laponite, MMT: montmorillonite, ZNT: zinc oxide nanotube, CVD: chemical vapor deposition, IL: ionic liquids, ChEt: cholesterol esterase, pRGOSHs: partially reduced graphene oxide–SiO$_2$ particle hybrid system, PAni–Au: polyaniline–gold nanocomposite.
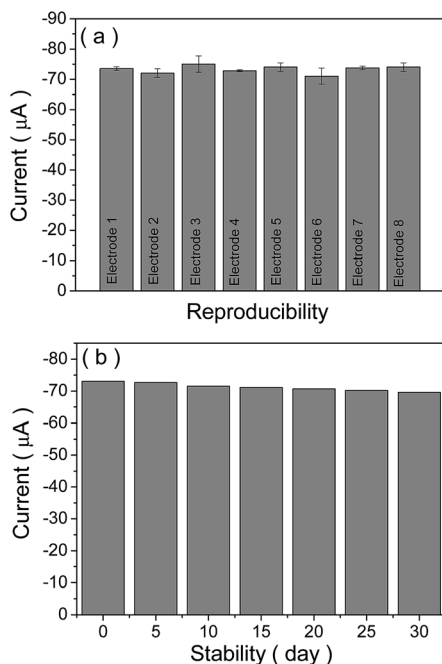
Fig. 7 The results of (a) reproducibility and (b) stability studies based on the ChOx/ZnO/Ag/GO–CS/ITO electrode were measured at a 50 mV s^{-1} scan rate in the presence of 200 mg dL^{-1} cholesterol solution.

Table 2 Determination of cholesterol concentration in real samples ($n = 3$)

Sample	Addition (mg dL^{-1})	Found (mg dL^{-1})	Recovery (%)	RSD (%, $n = 3$)
1	100	98.3	98.3	0.7
2	200	204.6	102.3	1.8
3	300	303.5	101.2	1.4

Real sample test

To test the potential application of the ChOx/ZnO/Ag/GO–CS/ITO electrode in real samples, recovery experiments were performed *via* the standard addition method under optimal conditions. Three different concentrations of cholesterol were added three times ($n = 3$) to a 200 mg dL^{-1} (5.2 mM) cholesterol solution. From Table 2, we could see acceptable recoveries and RSDs, indicating that the sensor could be efficiently used for the determination of cholesterol.

Conclusions

In this manuscript, we successfully immobilized ChOx on the surface of a ZnO/Ag/GO–CS functionalized ITO electrode. The combination of ZnO and AgNWs results in a low potential amperometric detection of cholesterol and excellent anti-interference ability of the biosensor. Amperometry techniques were used to detect the concentration of cholesterol solution on the ChOx/ZnO/Ag/GO–CS/ITO electrode. Our electrochemical measurements show that the developed electrode exhibited good catalytic performance with a wide linear range, low detection limit and high stability.

Acknowledgements

References

1 P. Holla, I. Ahmad, Z. Ahmed and S. Jameel, *Traffic*, 2015, **16**, 398.

2 J. I. Cleeman, *JAMA Intern. Med.*, 1988, **148**, 36.

3 K. Wakita, S. Morita, N. Okamoto, E. Takata, T. Handa and M. Nakano, *BBA, Biochim. Biophys. Acta, Mol. Cell Biol. Lipids*, 2015, **1851**, 598.

4 J. D. Brunzell, M. Davidson, C. D. Furberg, R. B. Goldberg, B. V. Howard, J. H. Stein and J. L. Witztum, *J. Am. Coll. Cardiol.*, 2008, **51**, 1512.

5 N. Agnihotri, A. D. Chowdhury and A. De, *Biosens. Bioelectron.*, 2015, **63**, 212.

6 A. Ahmadalinezhad and A. Chen, *Biosens. Bioelectron.*, 2011, **26**, 4508.

7 L. Xu, Y. Hou, M. Zhang, T. Cheng, W. Huang, C. Yao and Q. Wu, *Anal. Methods*, 2015, **7**, 5649.

8 H. Ditlbacher, A. Hohenau, D. Wagner, U. Kreibig, M. Rogers, F. Hofer, F. R. Aussenegg and J. R. Krenn, *Phys. Rev. Lett.*, 2005, **95**, 257403; J. Richter, M. Mertig, W. Pompe, I. Mönch and H. K. Schackert, *Appl. Phys. Lett.*, 2001, **78**, 536; X. Zhao, B. Zhang, K. Ai, G. Zhang, L. Cao, X. Liu, H. Sun, H. Wang and L. Lu, *J. Mater. Chem.*, 2009, **19**, 5547; R. J. Chimentão, I. Kirm, F. Medina, X. Rodríguez, Y. Cesteros, P. Salagreb and J. E. Sueiras, *Chem. Commun.*, 2004, **7**, 846.

9 D. T. Schoen, A. P. Schoen, L. Hu, H. S. Kim, S. C. Heilshorn and Y. Cui, *Nano Lett.*, 2010, **10**, 3628.

10 S. P. Singh, S. K. Arya, P. Pandey and B. D. Malhotra, *Appl. Phys. Lett.*, 2007, **91**, 063901; H. Kim, C. M. Gilmore, J. S. Horwitz, A. Piqué, H. Murata, G. P. Kushto, R. Schlaf, Z. H. Kafafi and D. B. Chrisey, *Appl. Phys. Lett.*, 2000, **76**, 259; T. Ghoshal, S. Kar and S. Chaudhuri, *J. Cryst. Growth*, 2006, **293**, 438; M. J. S. Spencer, *Prog. Mater. Sci.*, 2012, **57**, 437; H. Q. Chiang, J. F. Wager, R. L. Hoffman, J. Jeong and D. A. Keszler, *Appl. Phys. Lett.*, 2005, **86**, 013503; J. X. Wang, X. W. Sun, A. Wei, Y. Lei, X. P. Cai, C. M. Li and Z. L. Dong, *Appl. Phys. Lett.*, 2006, **88**, 233106; A. Umar, M. M. Rahman, S. H. Kim and Y.-B. Hahn, *Chem. Commun.*, 2008, **2**, 166; Y. Zhang, K. Yu, D. Jiang, Z. Zhu, H. Geng and L. Luo, *Appl. Surf. Sci.*, 2005, **242**, 212.

11 P. R. Solanki, A. Kaushik, A. A. Ansari and B. D. Malhotra, *Appl. Phys. Lett.*, 2009, **94**, 143901.

12 P. Nayak, B. Anbarasan and S. Ramaprabhu, *J. Phys. Chem. C*, 2013, **117**, 13202.

13 J. D. Fowler, M. J. Allen, V. C. Tung, Y. Yang, R. B. Kaner and B. H. Weiller, *ACS Nano*, 2009, **3**, 301.

14 A. M. Martins, G. Eng, S. G. Caridade, J. F. Mano, R. L. Reis and G. Vunjak-Novakovic, *Biomacromolecules*, 2014, **15**, 635.

15 T. Cheng, Y. Z. Zhang, W. Y. Lai, Y. Chen, W. J. Zeng and W. Huang, *J. Mater. Chem. C*, 2014, **2**, 10369.

16 J. Wang, N. Wang, Y. Jin, J. Si, Z.-K. Tan, H. Du, L. Cheng, X. Dai, S. Bai, H. He and Z. Ye, *Adv. Mater.*, 2015, **27**, 2311.

17 P. Nayak, B. Anbarasan and S. Ramaprabhu, *J. Phys. Chem. C*, 2013, **117**, 13202.

18 N. Batra, M. Tomar and V. Gupta, *Biosens. Bioelectron.*, 2015, **67**, 263.

19 E. Laviron, *J. Electroanal. Chem.*, 1979, **100**, 263.

20 M. Chaplin and C. Bucke, *Enzyme Technology*, Cambridge University Press, London, 1990, ch. IV.

21 N. Joshi, K. Rawat, P. R. Solanki and H. B. Bohidar, *Biochem. Eng. J.*, 2015, **102**, 69.

22 T. T. L. Souza, M. L. Moraes and M. Ferreira, *Sens. Actuators, B*, 2013, **178**, 101.

23 R. Khan, A. Kaushik, P. R. Solanki, A. A. Ansari, M. K. Pandey and B. D. Malhotra, *Anal. Chim. Acta*, 2008, **616**, 207.

24 R. Ahmad, N. Tripathy, S. H. Kim, A. Umar, A. Al-Hajry and Y.-B. Hahn, *Electrochem. Commun.*, 2014, **38**, 4.

25 A. Rengaraj, Y. Haldorai, C. H. Kwak, S. Ahn, K.-J. Jeon, S. H. Park, Y.-K. Han and Y. S. Huh, *J. Mater. Chem. B*, 2015, **3**, 6301.

26 N. Joshi, K. Rawat, P. R. Solanki and H. B. Bohidar, *Sensing and Bio-Sensing Research*, 2015, **5**, 105.

27 H. Dhyani, M. A. Ali, S. P. Pal, S. Srivastava, P. R. Solanki, B. D. Malhotra and P. Sen, *RSC Adv.*, 2015, **5**, 45928.

28 S. Abraham, S. Srivastava, V. Kumar, S. Pandey, P. K. Rastogi, N. R. Nirala, S. Kashyap, S. K. Srivastava, V. N. Singh, V. Ganesan, P. S. Saxena and A. Srivastava, *J. Electroanal. Chem.*, 2015, **757**, 65.

29 P. R. Solanki, A. Kaushik, A. A. Ansari, A. Tiwari and B. D. Malhotra, *Sens. Actuators, B*, 2009, **137**, 727.

30 M. Srivastava, S. K. Srivastava, N. R. Nirala and R. Prakash, *Anal. Methods*, 2014, **6**, 817.